

# Design and Dynamic Control of Fiber-Granular Routing Networks with Next-Generation Optical Paths

Takeshi Matsuo, Ryuta Shiraki, Yojiro Mori, Hiroshi Hasegawa

*Nagoya University, Furo-cho, Chikusa, Nagoya, 464-8603, Japan*

*matsuo.takeshi@a.mbox.nagoya-u.ac.jp*

**Abstract:** Efficient network design and control algorithms for fiber-granular routing networks are proposed. Routing performance of next-generation broad-bandwidth optical paths on fiber-granular routing networks with over 100×100 fiber-cross-connects is verified. © 2022 The Authors

## 1. Introduction

To cope with the steep and continuous growth in Internet traffic [1], which have even accelerated with the outbreak of COVID-19 [2], cost-effective expansion of optical network capacity is now crucial. While 100 Gbps transponders have been widely deployed, further bitrate improvement is demanded, with not only footprint and power consumption reduction but also simplification of network operations by decreasing the number of transponders used. Currently, 200/400 Gbps transponders using higher-order modulation and higher baud-rates are being commercialized. Moreover, beyond 1 Tbps transponders are being intensively developed [3]. These next-generation optical paths will occupy broader frequency ranges so each fiber will carry fewer paths.

The capacity of single-mode optical fibers (SMFs) is now approaching its upper limit [4]; as a result, the number of SMFs (or, equivalently, cores in multi-core fibers) laid on each link will inevitably increase due to the exploding traffic volume. The degrees of optical cross-connects at nodes will be several tens and cost-effective cross-connect configurations must be introduced. Current high-port count WSSs such as 1×35 allow conventional wavelength cross-connects (WXC) with path-by-path switching capability; that is, path-granular routing. The adoption of large-scale optical switches as fiber cross-connects (FXC) is being discussed recently as their degrees can be over 300 [5] and their signal power loss is generally less. Different from WSS-based cross-connects, all paths in an input fiber must be routed together to one of the output fibers; that is, fiber-granular routing. This property substantially constrains path routing flexibility; the impact will be more evident with adoption of the transport software-defined network (SDN) technology [6].

In path-granular routing networks, an optical path can select any route from its source to its destination. Moreover, the path can traverse any fiber on each link of the selected route provided the wavelength to be assigned is not used on the fiber. The statistical multiplexing effect is enhanced by the arbitrary selection of route and fiber. On the other hand, for fiber-granular routing networks, if a new path is assigned to a fiber carrying existing paths, there is no flexibility in the selection of the next link and fiber on the next link; the switching state of the FXC must remain fixed to avoid disrupting the services carried by the existing paths. The statistical multiplexing effect is limited due to inflexibility of routing. In addition, the decrease in the number of paths per fiber expected for next-generation 1+ Tbps paths further degrades the effect. Therefore, we have to clarify the routing performance of such paths on fiber-granular routing networks using large-scale FXCs.

In this paper, we first propose an efficient algorithm that simultaneously optimizes fiber arrangements and switching states in networks whose largest node scale exceeds 100×100. Then we explain how paths are dynamically operated on the designed networks. Finally, numerical simulations on real topologies are conducted, and the blocking ratio of path setups in networks with FXCs and those with WXC are evaluated. Replacing WXC with FXC decreases the traffic intensity values for the blocking ratio of  $10^{-3}$  by up to 57% and 52% for Pan-European and North American network topologies, respectively.

## 2. Sub-Network Arrangement and Dynamic Control of Fiber-Granular Routing Networks

This paper assumes fully transparent optical path networks with  $N$  nodes. Neither wavelength conversion nor 3R regenerator is used. In order to simplify the notations and discussions, we assume that path capacities are uniform and all paths occupy the same frequency bandwidth. However, the introduction of multiple path capacities and distance-adaptive modulation format selection is straightforward. The traffic demand distribution is characterized by matrix  $T$  whose  $(i, j)$  ( $i, j = 1, 2, \dots, N$ ) component represents the expected number of paths to be established from node  $i$  to node  $j$ .

The OXC node configurations assumed in this paper are shown in Fig. 1. Their path-granular add/drop parts are common to both configurations to highlight the difference between their express parts; FXCs and WXC. For WXC, cascaded multiple WSSs are assigned to each input/output fiber if the degree of the WXC exceeds that of available WSSs. For each input fiber, a FXC terminates all paths in an input fiber or assigns one of the output fibers exclusively to the input fiber to route all express paths together between the fiber pair. These

operations define sets of circular/linear chains of fibers in a network with FXCs where all paths are routed along the chains. Hereafter we call each chain a sub-network as shown in Fig. 2.

This paper compares FXC and WXC performance in two phases; initial network setup phase (Phase 1) and dynamic path operation phase (Phase 2). In Phase 1, given a topology and matrix  $T$ , a set of sub-networks is designed and fibers necessary for the sub-networks are laid on links. Then, in Phase 2, dynamic path setup/tear-down requests are generated between each node pair so that the expected number of paths will be a desired value, called traffic intensity, and the blocking ratio of path setup is observed. The algorithms developed for these phases are summarized below.

**Phase 1 (Initial setup):** Generate a set of path setup demands so that the number of paths between node  $i$  and node  $j$  is  $T(i, j)$ . Select a path demand, not processed yet, between  $(s, d)$  so that the number of hops of the shortest route from  $s$  to  $d$  is the largest. If there is a sub-network going through  $(s, d)$  with unused wavelength/spectrum, setup the path in the sub-network. Otherwise, find a disjoint route pair between  $s$  and  $d$  and establish a new sub-network on the route pair. Setup the path on the new sub-network. Repeat until all demands are processed.

**Phase 2 (Dynamic path operation):** Dynamic path setup requests are generated according to the Poisson process where path lifetime follows a negative exponential distribution. The source and destination nodes  $(s, d)$  of generated paths are randomly assigned with probability of  $T(s, d) / \sum_{(i, j)} T(i, j)$ . Each path setup request that arrives is processed as follows. Search for sub-networks covering the source and destination nodes and with unused wavelength/spectrum. Among these sub-networks, select the one minimizing the number of traversed links weighed with the current utilization levels of these links. Setup the path on the selected sub-network. After the lifetime of a path has passed, the path is torn down immediately.

#### Remarks

1. Even for networks with over 20 nodes whose largest scale exceeds  $100 \times 100$ , the calculation time of Phase 1 is short enough ( $< 1$  minute) to repeat multiple times to find better sub-network and fiber arrangements.
2. We have already proposed an integer linear programming (ILP) based switching state optimization algorithm for fiber-granular routing networks [7]. That work focused on the ultra-dense WDM transmission on current optical networks. The fiber-granular routing contributes to the alleviation of the spectrum narrowing at WSSs. The algorithm works well only for networks where few fibers are laid on each link (e.g., 1-3 fibers/link); however, it is not applicable to next-generation optical networks that use many fibers. In Sec. 3.1, we will show the performance gap between the proposed and ILP-based methods is small.

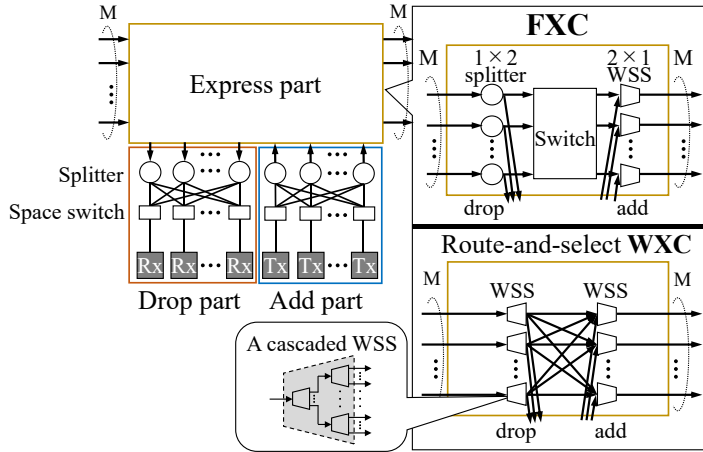


Fig. 1. WXC-based and FXC-based node configurations.

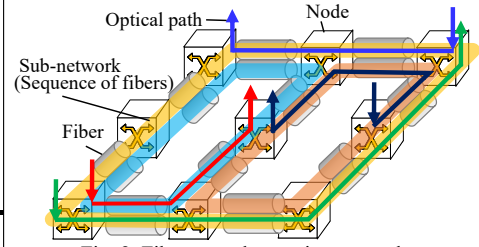


Fig. 2. Fiber-granular routing network.



Fig. 3. Examined network topologies.

### 3. Simulations

#### 3.1. Evaluation of The Optimality of Designed Sub-Networks

The optimality of sub-networks designed by the proposed method was evaluated by comparing the numbers of fibers and sub-networks given by the proposed and the ILP-based methods. The latter minimizes the number of fibers and works well only for small scale networks with small traffic volume. The 11-node Kanto (Tokyo metropolitan) topology [8] in Fig. 3 was used and the maximum number of optical paths per fiber  $C$  was set to 96. The number of paths between each node pair was changed from 1 to 7. Phase 1 in Sec. 2 was repeated 30,000 times to find a better sub-network set. Figure 4 shows the numbers of fibers and sub-networks. The proposed methods gave sub-optimal sub-networks with small fiber increment over the optimal sub-networks.

### 3.2. Performance Evaluations in Dynamic Path Operation Scenarios

Impact of the introduction of FXCs and broader bandwidth paths is evaluated in terms of path blocking probability. Physical network topologies tested are the COST266 Pan-European network with 26 nodes and 51 links and the USNET with 24 nodes and 42 links in Fig. 3 [9,10]. The maximum number of optical paths per fiber,  $C$ , was set to 25 and 3, which respectively represent 1 Tbps paths [3] and future paths such as 10 Tbps ones located in the C (+L) Band. The two node configurations shown in Fig. 1 were adopted. The number of optical paths between each node pair  $T(i, j) = \tau$  is the same for all node pairs; that is, a uniform traffic distribution is assumed.

Fiber and sub-network configurations were designed by setting  $(C, \tau) = (25, 6)$ ,  $(25, 12)$  and  $(C, \tau) = (3, 2)$ . The designed fiber configurations were used in common for both FXCs and WXC. The largest WXC/FXC for these configurations were  $44 \times 44 / 84 \times 84 / 131 \times 131$  (Pan-European) and  $36 \times 36 / 69 \times 69 / 101 \times 101$  (USNET), respectively. Then in the dynamic path operation phase, the expected number of paths established between each node pair was changed by controlling the path arrival rate following a Poisson process.

Figure 5 plots overall blocking ratio variations on the Pan-European network in terms of traffic intensity for path-granular and fiber-granular routing networks when  $(C, \tau) = (25, 12)$ . The traffic intensity achieving the target blocking ratio of  $10^{-3}$  for fiber-granular routing network was 48% smaller than that for path-granular routing networks. The traffic intensity values achieving the target blocking ratio for all configurations on two topologies are shown in Fig. 6 where the values are normalized with the  $\tau$  used in sub-network design. The introduction of FXCs decreases the traffic intensity values achieved by up to 51% for  $C = 25$  and 57% for  $C = 3$  which elucidates the severe degradation in the statistical multiplexing effect, especially for future paths.

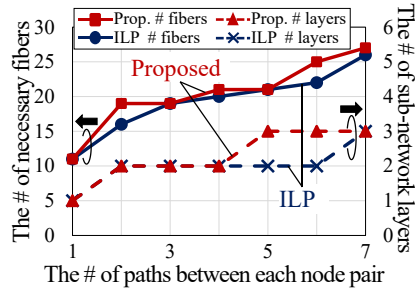


Fig. 4. The number of necessary fibers and sub-network layers.

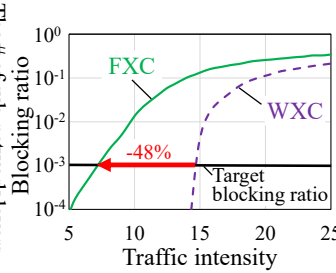


Fig. 5. Blocking-ratio variations on Pan-European when  $(C, \tau) = (25, 12)$ .

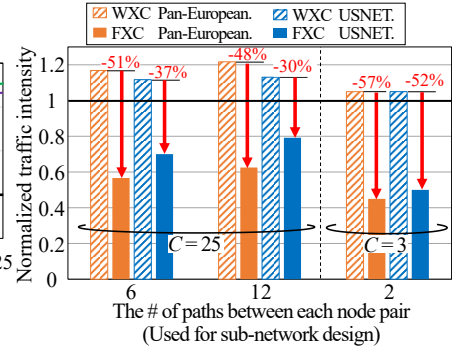


Fig. 6. Traffic intensity values that achieve the target blocking ratio of  $10^{-3}$  (Normalized by  $\tau$ ).

## 4. Conclusion

We have developed efficient network design and control algorithms for fiber-granular routing networks with path-granular add/drop. The severe degradation in statistical multiplexing effect was verified for the dynamic operation of future broad-bandwidth optical paths on fiber-granular routing networks with over  $100 \times 100$  FXCs. These results elucidated the substantial contribution of wavelength selectivity to path routing and the importance of electrical/optical multi-layer design and control in fiber-granular routing networks.

**Acknowledgment:** This work was partly supported by KAKENHI (20H02150).

## 5. References

- [1] Cisco System, Inc., "Cisco visual networking index: Forecast and methodology, 2017–2022 white paper,"
- [2] Ministry of internal affairs and communications, Telecommunications division data communication section, Jul. 21st, 2021. [Online]. [http://www.soumu.go.jp/main\\_content/000761096.pdf](http://www.soumu.go.jp/main_content/000761096.pdf), Last retrieved: Oct. 1st, 2021.
- [3] Workshop "Are 200+ Gbaud transmission systems feasible? The path to beyond 1 Terabit/s optical channels," ECOC, Mo3B-WS (2021).
- [4] P. J. Winzer, "Scaling optical fiber networks: Challenges and solutions," OSA Optics and Photonics News **26**, 28-35 (2015).
- [5] Polatis, <https://www.polatis.com/series-7000-384x384-port-software-controlled-optical-circuit-switch-sdn-enabled.asp>, Accessed: Oct. 1st, 2021.
- [6] Ramon Casellas *et al.*, "Advances in SDN control for beyond 100G disaggregated optical networks," ECOC, Tu1E.1 (2021).
- [7] R. Shiraki *et al.*, "Design and control of highly spectrally efficient photonic networks enabled by fiber-granular routing on overlaid ring-shaped topologies," IEEE/OSA Journal of Optical Communications and Networking **13**, 233-243 (2021).
- [8] Y. Hirota, "[Invited Talk] A study on Japan photonic network model and spatial division multiplexed elastic optical networks," IEICE Technical Report, PN2019-29 (2019).
- [9] N. Wauters *et al.*, "Design of the optical path layer in multiwavelength cross-connected networks," IEEE Journal on Selected Areas in Communications **14**, 881-892 (1996).
- [10] A. Nag *et al.*, "Optical network design with mixed line rates," Optical Switching and Networking **6**, 227-234 (2009).